Translational Oncology 29 (2023) 101628

Contents lists available at ScienceDirect

Translational Oncology

journal homepage: www.elsevier.com/locate/tranon

CKAP4-mediated activation of FOXM1 via phosphorylation pathways regulates malignant behavior of glioblastoma cells

Kaiyue Xu [a], Kaiqian Zhang [a,b], Jiying Ma [a], Qianqian Yang [a], Ge Yang [a], Tingting Zong [a], Guowei Wang [a,c], Bo Yan [a], Jule Shengxia [a], Chao Chen [a], Liang Wang [d,*], Huijuan Wang [a,*]

[a] National Engineering Research Center for Miniaturized Detection Systems, College of Life Sciences, Northwest University, Xi'an, Shaanxi, China
[b] Key Laboratory of Resource Biology and Biotechnology in Western China, Ministry of Education, Northwest University, Xi'an, Shaanxi, China
[c] Provincial Key Laboratory of Biotechnology of Shaanxi Province, Northwest University, Xi'an, Shaanxi, China
[d] Department of Neurosurgery, Tangdu Hospital of Fourth Military Medical University, 569 Xinsi Road, Xi'an, Shaanxi, China

ARTICLE INFO

Keywords:
Proteomics
Glioblastoma
CKAP4
Phosphorylation
FOXM1

ABSTRACT

Objective: CKAP4 (Cytoskeleton Associated Protein 4) has been reported as an important regulator of carcinogenesis. A great deal of uncertainty still surrounds the possible molecular mechanism of CKAP4 involvement in GBM. We aimed to specifically elucidate the putative role of CKAP4 in the development of GBM.

Methods: We identified divergent proteomics landscapes of GBM and adjacent normal tissues using mass spectrometry-based label-free quantification. Bioinformatics analysis of differentially expressed proteins (DEPs) led to the identification of CKAP4 as a hub gene. Based on the Chinese Glioma Genome Atlas data, we characterized the elevated expression of CKAP4 in GBM and developed a prognostic model. The influence of CKAP4 on malignant behavior of GBM was detected in vitro and vivo, as well as its downstream target and signaling pathways.

Results: The prognosis model displayed accuracy and reliability for the probability of survival of patients with gliomas. CKAP4 knockdown remarkably reduced the malignant potential of GBM cells, whereas its overexpression reversed these effects in GBM cells and xenograft mice. Moreover, we demonstrated that overexpression of CKAP4 leads to increased FOXM1 (Forkhead Box M1) expression in conjunction with an increased level of AKT and ERK phosphorylation. Inhibition of both pathways had synergistic effects, resulting in greater effectiveness of inhibition. CKAP4 could reverse the deregulation of FOXM1 triggered by inhibition of AKT and ERK signaling.

Conclusions: This is the first study to reveal a CKAP4-FOXM1 signaling cascade that contributes to the malignant phenotype of GBMs. The CKAP4-based prognostic model would facilitate individualized treatment decisions for glioma patients.

Introduction

Glioblastoma (GBM) represents one of the most lethal primary brain tumors in adults, characterized by high aggressiveness and dismal prognosis [1–3]. To date, the mechanism of GBM tumorigenesis is still not fully revealed. Despite the current standard-of-care treatment the surgery followed by radiotherapy and chemotherapy with the alkylating agent temozolomide (TMZ), the high-grade gliomas have a propensity to rapidly deteriorate and potentially lead to recurrence at 8-9 months following initial therapy [4–6]. Further exploration of the new mechanism of GBM to identify more effective therapeutic targets and develop efficient prognostic methods is helpful to improve the treatment efficacy of GBM patients.

CKAP4 (Cytoskeleton Associated Protein 4) is a type II transmembrane protein located in the endoplasmic reticulum (ER) membrane [7–9]. An accumulating body of evidence has suggested that CKAP4 functions as a positive regulator in the development of carcinogenesis, regulating phenotypes such as proliferation, migration and invasion [8, 10–13]. In addition, CKAP4 serves as a receptor for several ligands, including Dickkopf1 (DKK1). By activating downstream molecules of the AKT and PI3K-AKT pathways, CKAP4 stimulated cell proliferation by binding to DKK1 [14–17]. There is evidence that CKAP4 associated with

* Corresponding authors.
E-mail addresses: drwangliang@126.com (L. Wang), whj@nwu.edu.cn (H. Wang).

https://doi.org/10.1016/j.tranon.2023.101628
Received 22 October 2022; Received in revised form 27 December 2022; Accepted 16 January 2023

angiogenesis has a stronger intensity in high-grade gliomas as compared to low-grade gliomas [18].

FOXM1 (Forkhead Box M1), a transcription factor belonging to the FOX family, contributes to the proliferation, invasion, and epithelial-mesenchymal transition (EMT) of cancer cells [19,20]. The dysregulation of FOXM1 expression also interferes with the expression of genes involved in drug efflux and DNA repair [21]. Moreover, FOXM1 directly or indirectly activates the expression of target genes at the transcriptional level, whose dysregulation is implicated in almost all hallmarks of tumor cells [22,23]. For example, FOXM1 functions as an up-regulator of glycolysis genes through direct binding to the promoter of glycolysis genes [24–26].

Here, through the proteomic characterization of GBM tissues, we identified CKAP4 as a hub gene associated with GBM malignancy. The analysis of our data suggested that CKAP4 and FOXM1 were both upregulated in GBM, and their overexpression was correlated with a malignant phenotype and poor prognosis. Moreover, a series of in vitro and in vivo experiments showed that CKAP4 regulated FOXM1 expression through enhanced activation of both AKT and ERK pathways, which in turn promoted a malignant phenotype. Additionally, we developed a nomogram for predicting the prognosis of patients with gliomas based on the retrospective analysis of CGGA mRNA sequencing data. Proteomics-based identification of the potentially regulated pathways of CKAP4 and construction of the proposed nomogram might offer significant insight into the complicated biochemical processes underlying glioma biology, as well as a more accurate assessment of glioma risk.

Materials and methods

Clinical specimens

Resected tissue samples were obtained from patients pathologically diagnosed as GBM according to WHO criteria in the Tangdu Hospital, Second Affiliated Hospital of the Air Force Medical University. The Ethics Committee of the Fourth Military Medical University approved the study, and all patients have signed an informed consent form.

Label-free quantitative

The frozen brain tissues were denatured and reduced, then alkylated in the dark. Protein pellets solution was digested by sequencing grade trypsin (protein: enzyme, 100:1; Promega, USA). The trypsin-digested peptides were desalted, activated, and eluted. The peptide concentration was measured by bicinchoninic acid (Beyotime, China). Equal amounts of tryptic peptides were separated by an Easy-nLCTM 1200 system (Thermo Fisher Scientific, Germany) with the use of Acclaim PepMap100 precolumn (2 cm, 75 μm i.d., 3 μm) and Acclaim PepMap100 separating column (50 cm, 75 μm i.d., 3μm). The analysis was performed on an Orbitrap Fusion Lumos mass spectrometer (Thermo Fisher Scientific, Germany).

Protein identification and qualification

Data of global proteins were searched using SEQUEST in Proteome Discover 2.3 (Thermo Scientific) against the Uniport human protein databases downloaded from http://www.uniprot.org in June 2019. Peptides were searched with up to two missed cleavages after trypsin digestion. Global protein data analysis was filtered with a 1% false discovery rate threshold. The mass spectrometry proteomics data have been deposited to the ProteomeXchange Consortium (http://proteomecentral.proteomexchange.org) via the iProX partner repository with the dataset identifier PXD026503.

Hub gene screened and determined

The Kyoto Encyclopedia of Genes and Genomes (KEGG) enrichment of DEPs was displayed in Database for Annotation, Visualization, and Integrated Discovery (DAVID) (https://david.ncifcrf.gov/home.jsp). The protein-protein interaction (PPI) network and hub genes screened were established in STRING: functional protein association networks (https://string-db.org) and Cytoscape. The expression data of hub genes was searched in three databases, Gene Expression Profiling Interactive Analysis (GEPIA, http://gepia.cancer-pku.cn), UALCAN (http://ualcan.path.uab.edu) and Human Protein Atlas (HPA, http://v13.proteinatlas.org/).

Western blot

Samples were lysed in the RIPA buffer (HAT, China) in the presence of 1% PMSF and 1% inhibitor. Equal amounts of total protein were separated on 10% SDS-PAGE gradient gels and transferred to PVDF membranes. Membranes were blocked with 5% skim milk and then incubated with primary antibodies at 4℃ overnight, then incubated with secondary antibody. Blots were washed and analyzed on Image System (ENFAN-BIAS2600, China).

Cell culture and drug treatments

The GBM cell lines A172 (Procell, China) and U87 MG (American Type Culture Collection, USA) were cultured with a high-glucose DMEM medium containing 10% fetal bovine serum (FBS). Both cells were cultured in an incubator at 37℃ and supplied with 5% CO_2. AKT inhibitor VIII (HY-10355) and Mirdametinib (HY-10254) were purchased from MedChemExpress (USA).

Transient transfection and construction of stable cell lines

The siRNA targeting CKAP4 and control siRNA was synthesized by GenePharma (Shanghai, China), and shRNA targeting FOXM1 was the sequences were shown in Table S1. 80% of confluent cells were transfected with 50 nM siRNAs using Lipofectamine 2000 (Invitrogen, USA).

Lentiviral vectors encoding CKAP4 gene was constructed in Plenti-SFFV-P2A-puromycin (Genecarer, China). The U87 and A172 cells were seeded in 12-well plates, and infected with lentivirus-expressing CKAP4 or a negative control at 60 % confluence. After infection for 72 h, puromycin-resistant cell pools were identified by western blot after being screened with 1 μg/mL (U87) and 0.5 μg/mL (A172) polybrene (Beyotime, China).

CRISPR/Cas9 was applied to construct the recombinant vectors knocking out CKAP4 gene (Genecarer, China). The U87 and A172 cells were seeded in 12-well plates, and cells were transfected with the plasmid at 80 % confluence. After being transfected for 48 h, cells were treated with appropriate concentrations of polybrene. The puromycin-resistant cell pools were collected and identified by qPCR or WB.

Quantitative real-time PCR

According to the manufacturer's instructions, total RNA was extracted from cells by Trizol reagent. 1μg of RNA was reverse transcribed by TransScript All-in-One First-Strand cDNA Synthesis SuperMix (TransGen Biotech, China). The mRNA levels of CKAP4 were detected by quantitative real-time PCR (qRT-PCR) using PerfectStartTM Green qPCR SuperMix (TransGen Biotech, China), normalized to GAPDH. Sequences of primers were presented in Table S2. All mRNA expression levels were calculated using the $2^{-\Delta\Delta Ct}$ method and normalized to control.

Cell proliferation, migration, and invasion assays

For cell proliferation, cells were seeded at 5×10^4 per well in 96-well plates for 24 h, 48 h, and 72 h. The absorbance was measured at 490 nm after 10 μL CCK8 was added to each well. For the migration assay, 8 μm pore sized plain transwell inserts were placed in the matched 24-well

plates. Cells in the FBS-free medium were inoculated into the upper chamber, while the bottom chamber was filled with a medium containing 10 % FBS. For the invasion assay, the procedure was the same as above except for the upper chambers pre-coated with matrix gel (Corning Costar, USA). After 24 h, cells on the topside of the chamber were manually removed with a cotton swab. Cells adherent to the undersurface of the insert were fixed in 4 % paraformaldehyde for 15 min and then stained with 0.1% crystal violet solution for 10 min. After the filters were washed in PBS, images were taken and countered using Image J.

Preparation of cytosolic and nuclear protein

Cytosolic and nuclear protein were prepared by the Nuclear Protein Extraction Kit (Solarbio, China) according to the manufacture's instruction. The antibody information was presented in Table S3.

Immunofluorescence

Cells were plated on confocal dishes for 24 h before being fixed with 4 % paraformaldehyde for 30 min and permeabilized with 0.5 % Triton X-100 for 20 min. Cells were blocked with 1 % BSA and 0.05 % Tween-20 for 30 min at room temperature. Following an overnight incubation with primary antibody at 4 ℃ overnight, an Alexa fluor 594-conjugated secondary antibody and 1μg/mL DAPI were used. The confocal microscopy was utilized to capture images (Leica, Germany).

In vivo tumorigenicity

The male athymic BALB/c nude mice (five-weeks-old) purchased from Vital River Laboratories (Beijing, China) were divided into two groups (n= 5/group). Approximately 1×10^7 CKAP4 overexpression-U87MG or control cells were subcutaneously injected to establish a tumor xenograft model. We measured tumor size every 2 days using calipers starting on day 4 post-injection. Tumor volume was calculated using the formula: length$\times$width$^2\times$0.5236. After 14 days, the mice were sacrificed, and the tumors were isolated. All animal experiments were approved by the Northwest University Animal Ethics Committee.

Immunohistochemistry

Paraffin-embedded tissue sections were deparaffinized and rehydrated, followed by endogenous peroxidase activity quenched and antigen retrieval performed. Standard protocol was followed to prepare tissue samples for immunohistochemical (IHC) staining using the primary antibody. Slides incubated with HRP conjugated anti-rabbit secondary antibody, followed by DAB and counterstained with hematoxylin, subsequently observed under a light microscope.

Data collection from CGGA

The Chinese Glioma Genome Atlas (CGGA, http://www.cgga.org.cn/) was used to obtain the mRNA expression profiles and matching clinical data of 1018 glioma patients and 20 non-gliomas patients. We utilized the ComBat function of the sva package to eliminate batch effects from glioma samples from two batches. Except for cases with insufficient or erroneous information, the investigation finally comprised 442 individuals with pathologically diagnosed gliomas and 20 patients without gliomas.

Data analysis

The quantitative data between subgroups were compared using Student's t-test. The survival rates were evaluated using the Kaplan-Meier method and compared by the log-rank test. The statistical analysis was performed using SPSS 19.0 software.

The Cox proportional hazard model was used to do multivariate analysis on the prognosis of patients with glioma to determine the independent risk factors. The Schoenfeld residuals were used to evaluate the proportional hazard (PH) assumption. A time-dependent covariate Cox regression model would be established if the Cox model doesn't conform to the PH assumption. The time was processed in segments, and the time-dependent covariates were stratified according to time segmentation. The median overall survival was taken as the cutting point, followed by a new Cox regression model constructed. Based on the significantly different variables filtered from the multivariate logistic regression model, a nomogram model was constructed using the R studio package of "rms" to quantify the relationship between CKAP4 levels as well as clinical parameters and survival probability (1-year, 2-year, and 3-year). The performance of the nomogram was evaluated by calibration curves and the area under the receiver operating characteristic curve, followed by validation. $P < 0.05$ was considered to have a significant difference among each group.

Results

Identification and characterization of DEPs and hub genes in GBM

We performed label-free mass spectrometry (MS) among GBM and adjacent tissues, three cases in each group (Fig. 1A). The research contoured the proteomic landscape in a deep level of coverage by quantifying 5737 proteins. The comparison of GBM to normal control revealed that 99 proteins (2.2%) were upregulated, some by as much as 25 times, and 466 proteins (10.5%) were downregulated (Fig. 1B). The constructed PPI network of 99 upregulated proteins contained 82 nodes and 262 edges (Fig. 1C). According to the MCC method under the scores level, the top 10 genes were P4HB, PDIA6, DNAJC3, LGALS1, CKAP4, F5, FGG, FGA, CALR, and CANX (Fig. 1D, Table S4). KEGG pathway analysis for ten hub genes mainly involves post-translational protein phosphorylation (Fig. 1E).

Validation of hub gene expression using databases

Gene expression profiles for hub genes were largely validated using the GEPIA, UALCAN, and HPA databases. From the GEPIA database, seven potential essential genes were found to be upregulated in gliomas (P4HB, PDIA6, DNAJC3, LGALS1, CKAP4, CALR, and CANX) (Fig. 2A). Based on the UALCAN database, the remaining genes also showed a higher expression in glioma, except for DNAJC3 (Fig. 2B). The protein levels of DNAJC3, as well as PDIA6, LGALS1, CKAP4, and CANX, were elevated within the HPA dataset (Fig. 2C). After integrating the information discussed above, we selected four genes (PDIA6, LGALS1, CKAP4, and CANX) and excluded those with inconsistent data. Considering that the function of PDIA6 and LGALS1 in gliomas has been extensively studied [27,28], they were excluded in the following analysis. Then, the clinical relevance of CKAP4 and CANX in GBM has been investigated in the CGGA database. CANX had no effect on survival probability ($P > 0.05$), whereas CKAP4 had a negative effect on survival probability ($P < 0.05$) (Fig. 2D). Then, we validated the level of CKAP4 expression in four random or paired samples of tissue samples, which was in line with the mass spectrometric results (Fig. 2E).

The development of a predictive nomogram based on independent risk factors

In a retrospective analysis of 442 glioma specimens, we performed univariate analyses to identify independent factors for survival. The results revealed that the following factors were associated with poor clinical outcome: high expression of CKAP4, high grade, advanced age, non-chemotherapy, IDH wildtype, non-codeletion of X1p19q, and unmethylated MGMT promoter (Table 1). Patients with a high level of CKAP4 had a shorter overall survival time (Fig. 3A). In a multivariate

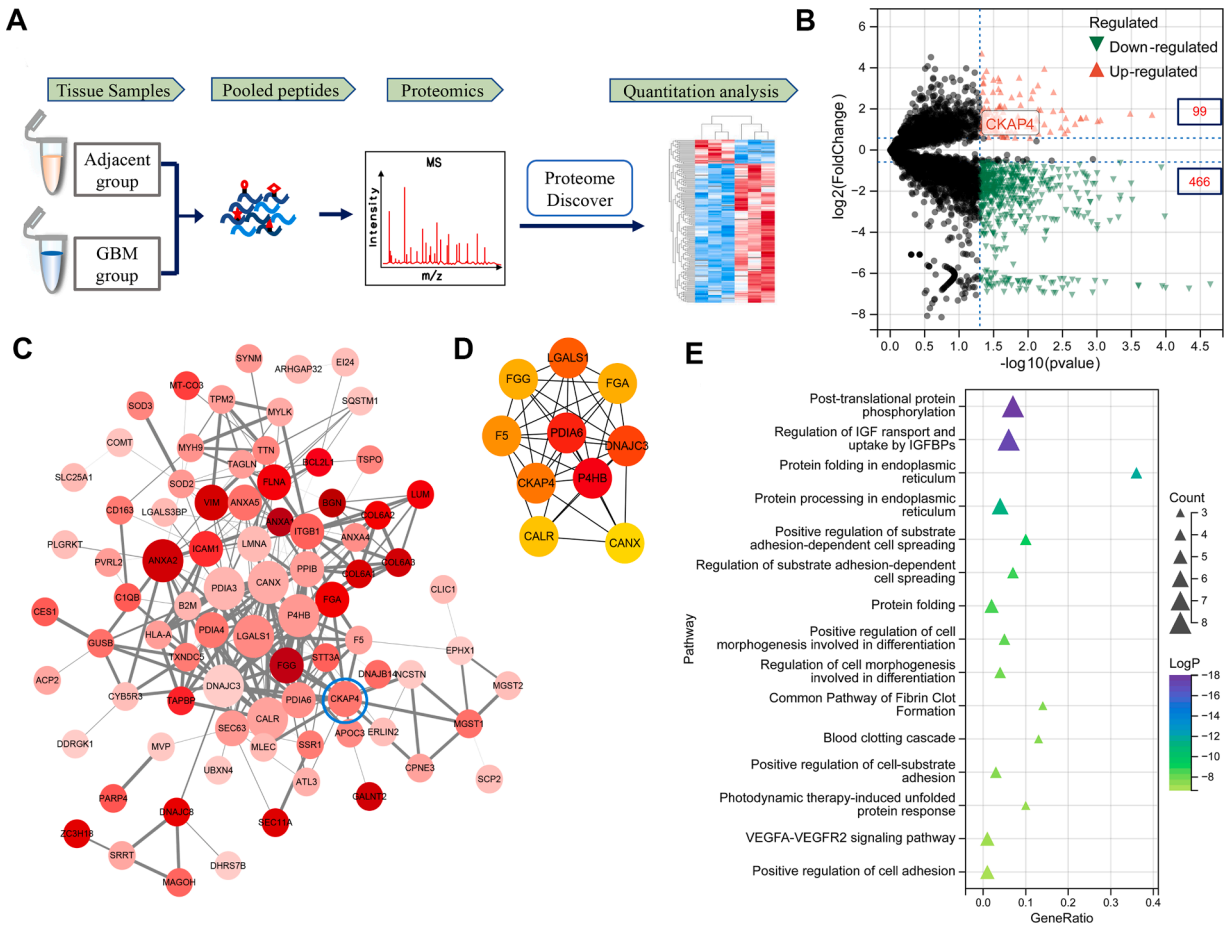

Fig. 1. Identification and screening of differentially expressed proteins (DEPs) and hub genes in GBM. (A) Workflow of quantitative proteome analysis for GBM and adjacent tissues. (B) Volcano plot of DEPs in GBM. The red dots represent upregulated proteins identified based on $\log_2$(fold change) ≥ 1 and $P < 0.05$. The green dots indicate the proteins that have been downregulated based on $\log_2$(fold change) ≤ -1 and $P < 0.05$. The grey dots represent proteins with no significant difference ($P > 0.05$). The black dots show proteins with $P < 0.05$ while $-1 < \log_2$(fold change) < 1. (C) Protein-protein interaction (PPI) network for the 99 upregulated proteins in GBM using Cytoscape. The rise in protein expression levels from low to high was denoted by the color change from pink to red. The size of the circle was inversely proportional to the number of edges with which nodes were connected. The thickness of the edge represented the sum of the linked node's scores, which was likewise positively correlated. (D) Hub genes identified in the top-scoring module from the PPI network. (E) KEGG pathways of the ten hub genes mainly enriched.

Cox regression analysis, CKAP4 overexpression was still identified as a substantial independent risk factor for poor prognosis (Table S5). The results of proportional hazard (PH) assumption indicated a notable statistical difference in the three covariates of grade, IDH, and X1p19q, together with the overall test of the model ($P < 0.05$) (Fig. S1), and the Cox model didn't conform to the PH assumption. Consequently, a time-dependent covariate Cox regression model was developed. The segmented model revealed that each covariate and the entire model met the PH assumption ($P > 0.05$). Considering that the average survival time of glioma patients is only 15 months [6], we constructed the short-term model to predict the prognosis. Based on the short-term model, CKAP4 high expression was a noteworthy independent risk factor for survival of glioma patients ($P < 0.05$) (Table 2, Fig. 3B).

Based on the c-index of 0.828, the nomogram performed extremely well in the prediction task. The area under the curve (AUC) for 1-year survival was 0.81, 0.88 for 2-year survival, and 0.89 for 3-year survival, indicating that the prediction was accurate (Fig. 3C). According to Fig. 3D, the survival rate of patients significantly decreased following the increase in risk scores. Multiple risk factors were observed, including high grade, advanced age, lack of chemotherapy, IDH wildtype, and non-codeletion of X1p19q. As indicated by the calibration curve, the predicted probability was relatively close to the actual probability value (Fig. 3E). An external database validation of the nomogram was conducted by evaluating its calibration curve using mRNA microarray data from CGGA, demonstrating the reliability of the predictive model (Fig. 3F).

CKAP4 enhanced the malignant characteristics of GBM cells

To investigate the biological function of CKAP4, we incorporated studies with siRNAs targeting CKAP4 (siRNA-CKAP4) in U87 and A172 cells, which demonstrated effective knockdown of the protein and mRNA (Fig. 4A, B). According to our data, knockdown of CKAP4 significantly inhibited proliferation in U87 and A172 cells (Fig. 4C). In addition, the migration and invasion capacity of U87 and A172 cells was also suppressed by knockdown of CKAP4 (Fig. 4D). In contrast, overexpression of CKAP4 promoted the proliferation, migration, and invasion of U87 and A172 cells (Fig. 4E, F, G). We also explored the influence of CKAP4 on tumor growth in nude mice, and the xenograft tumor volume triggered by CKAP4 overexpression-U87 cells was obviously large contrasted to the control group (Fig. 4H, Fig. S2). Ki-67 staining in xenograft tumors further supported the above conclusions (Fig. 4I). These results demonstrate that CKAP4 promotes the malignant properties of GBM cells as a positive regulator.

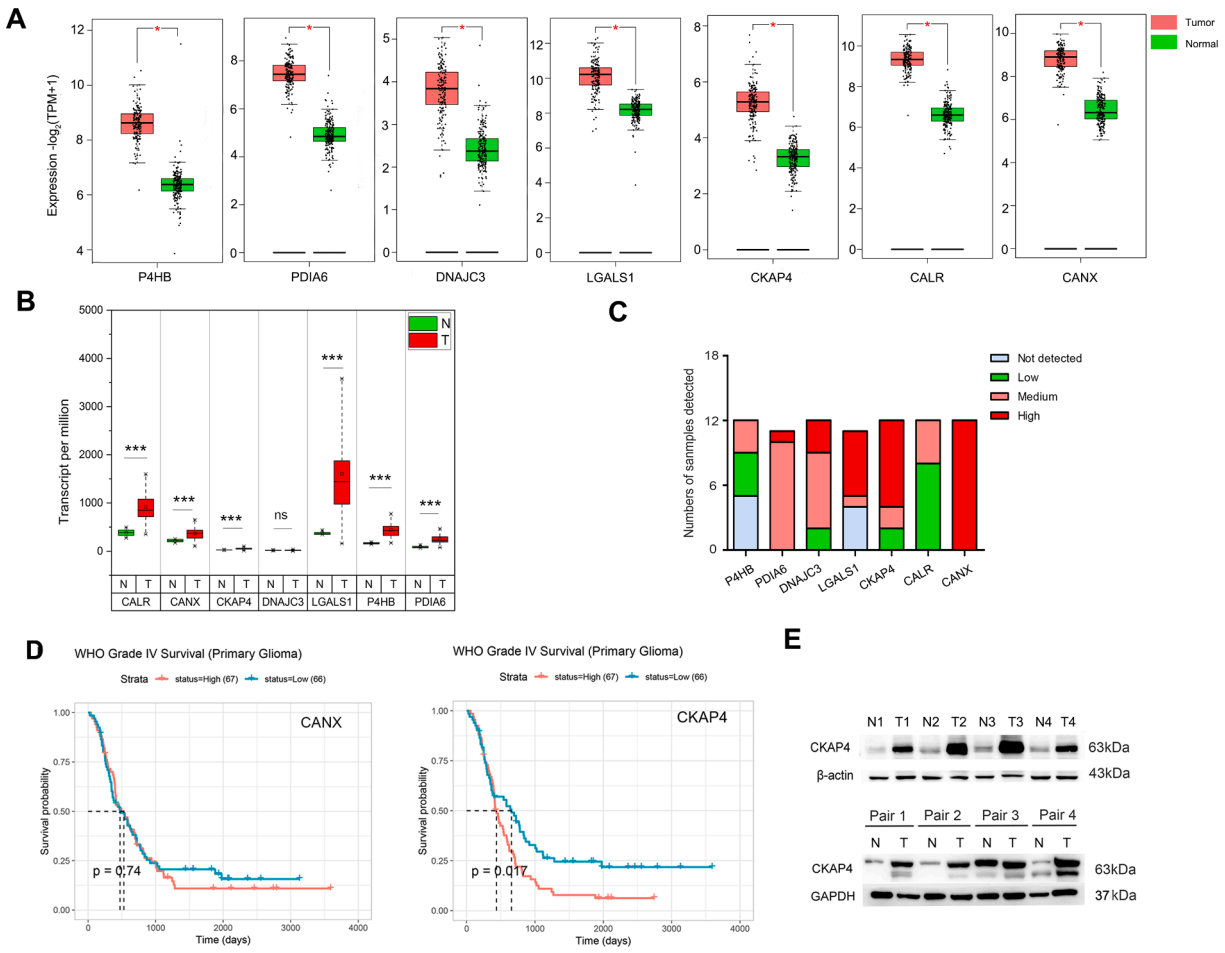

Fig. 2. Database-based expression of hub genes and overexpression of CKAP4 verified in GBM. (A) Transcription levels of seven hub genes were found highly expressed in GBM tissues contrasted to normal tissues with a cutoff value $|\log_2 FC|=1$ ($P < 0.01$) in the GEPIA database. The red box represents the expression of genes in the tumor group, whereas the green box indicates the expression of genes in normal control. (B) In the UALCAN database, the transcriptional levels of seven hub genes were shown to be strongly expressed in GBM except for DNAJC3 ($P < 0.001$). N: normal tissue; T: tumor. (C) The HPA database was examined for the translational level of seven hub genes expression in GBM. The percentage of samples with moderate or high expression is displayed above the column. Five hub genes were discovered to be highly expressed in more than 50% of GBM samples. (D) The correlation between CANX and CKAP4 expression and prognosis in glioma patients (data downloaded from CGGA datasets). (E) Western blot analysis reveals increased expression of CKAP4 in four randomly selected or matched GBM tissue samples. N: normal tissue; T: GBM. *$P < 0.05$, **$P < 0.01$, ***$P < 0.001$.

CKAP4 induces oncogenesis through post-transcriptional activation of FOXM1

There is evidence that the DKK1-CKAP4 pathway is essential for FOXM1 expression, and that CKAP4 knockdown reduced FOXM1 expression, which was rescued by restoring CKAP4 expression [29]. FOXM1 expression was elevated in GBM as compared to the normal tissues and was associated with a poor prognosis [30]. According to data provided by the CGGA, the upregulation of FOXM1 and its correlation with short overall survival agreed with the data provided above (Fig. S3). Furthermore, we observed a high expression of CKAP4 and FOXM1 in GBM (Fig. 5A). Moreover, patients with high CKAP4 and FOXM1 levels have a lower survival probability than those with high expression of either gene (Fig. 5B). As a result, we speculate that CKAP4 activates FOXM1 expression to enhance the malignant biological properties.

Interestingly, overexpressed CKAP4 significantly induced an elevated FOXM1 protein level in U87 and A172 cells. On the contrary, inhibition of CKAP4 drastically reduced FOXM1 protein level (Fig. 5C, Fig, S4 and S5). Nevertheless, neither knockdown or overexpressed of CKAP4 in U87 and A172 cells almost didn't cause changes of FOXM1 in transcription levels (Fig. 5D). To further confirm the effect of CKAP4 on FOXM1 expression, we detected the levels of FOXM1 in the nucleus and cytoplasm. The findings demonstrated that overexpression of CKAP4 didn't affect the cytosolic protein expression of FOXM1 in U87 and A172 cells, but significantly enhanced its expression in nuclei. Conversely, the decreased expression of CKAP4 in U87 and A172 cells reduced nuclear protein level of FOXM1, rather than its cytosolic protein level (Fig. 5E, Fig. S6). FOXM1 was labeled with red fluorescence, and its strong signaling was predominantly present in the nucleus of U87 and A172 cells in the presence of CKAP4 (Fig. 5F). The data indicate that CKAP4 facilitates post-transcriptional activation of FOXM1.

In line with aforementioned information, the result that increased FOXM1 protein levels in CKAP4 overexpressed xenograft tumors compared with control was corroborated (Fig. 2H, Fig. S7). Furthermore, we knocked down FOXM1 expression in CKAP4-overexpression U87 and A172 cells, and found that the ability of U87 and A172 cells to proliferate, migrate, and invade resulted by the overexpression of CKAP4 was reversed (Fig. 5G, H, I). These data reveal that CKAP4 potentiates oncogenesis through activation of FOXM1.

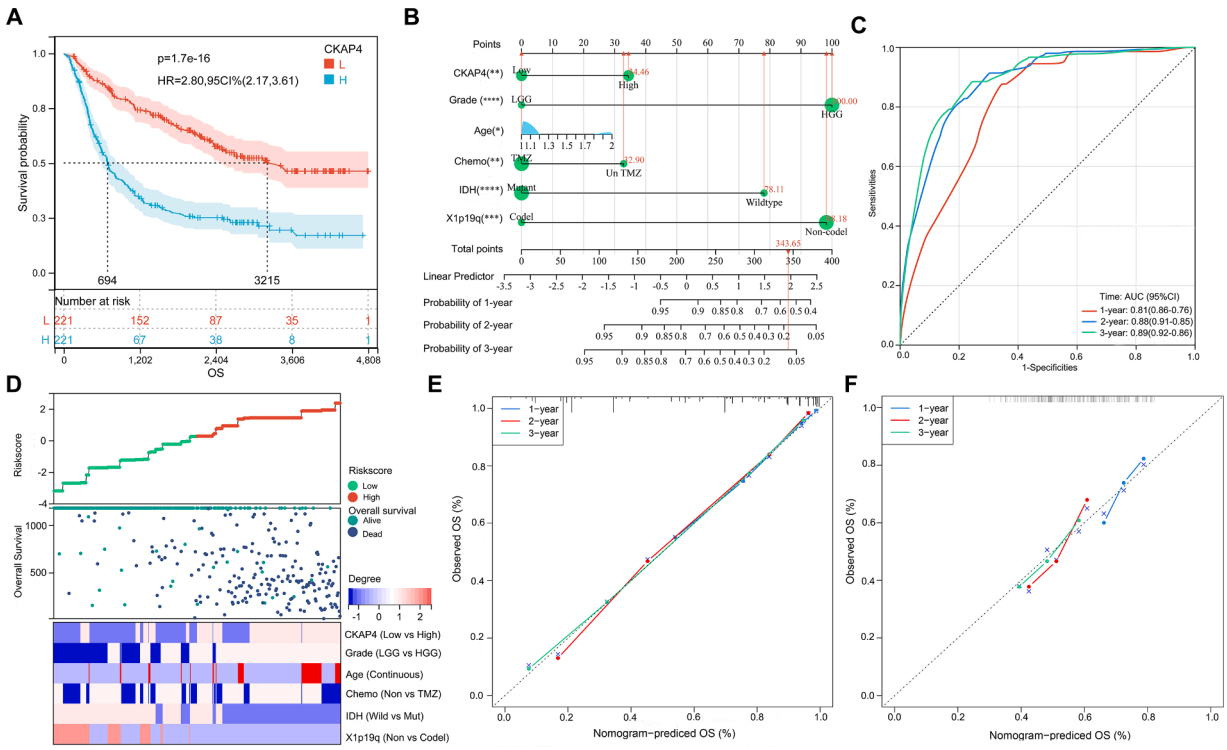

Fig. 3. A predictive nomogram based on independent risk factors. (A) Correlation analysis of CKAP4 expression from a retrospective analysis of 442 glioma specimens. (B) Relationship between the prognostic model and the variables in the model. The correlation between different risks scores and overall survival time, clinical parameters, and CKAP4 expression levels was shown. (C) The accuracy of the model was evaluated by the receiver operating characteristic (ROC) curve. (D) Short-term prognostic model Nomogram for predicting the probability of survival of glioma patients. The risk factors in different conditions represented a specific point, and the sum of these four elements represented the total number of points that could be used to predict the outcomes of each glioma patient. (E) The calibration curve was used to evaluate the discrepancy between the theoretical values and predictive values. (F) The calibration curve was used to evaluate the reliability of the predictive model from an external database.

CKAP4 regulates FOXM1 expression through the AKT/ERK signaling pathway

In the previous section, it was discussed that the KEGG pathways of the ten hub genes were mainly concerned with post-translational protein phosphorylation, and CKAP4 was included in the pathway (Fig. S8). AKT serine and threonine phosphorylation, coupled with the extracellular signal-regulated protein kinase (ERK) pathway are the important signaling events involved in cell proliferation and survival [31,32]. As a result of measuring the levels of phosphorylation of AKT and ERK, it was determined that overexpression of CKAP4 was associated with increased levels of phosphorylated AKT and ERK, and vice versa (Fig. 6A).

Researchers have found that PIK3/AKT regulates FOXM1 transcription via phosphorylation [33,34]. ERK directly phosphorylates FOXM1, which increases its nuclear translocation and transcription activity [35]. Therefore, we hypothesize that CKAP4 could modulate FOXM1 expression through activation of AKT and ERK pathways. First, we used different concentration gradients of the AKT inhibitor VIII as well as PD0325901 to prevent the activation of AKT and ERK. The results revealed that FOXM1 expression was dose-dependently reduced after treatment with AKT inhibitor VIII for 48 h in U87 cells, and markedly decreased after treatment with 10 μM AKT inhibitor VIII for 48 h in A172 cells (Fig. 6B). After treated with 2 μM PD0325901 for 48 h in both cells, we observed a significant inhibition of FOXM1 expression (Fig. 6C). When U87 and A172 cells were concurrently treated with AKT inhibitor VIII and PD0325901 for 48 h, we found the combining inhibition of the AKT and ERK pathways had synergistic effects and increased the effect of the inhibition on FOXM1 expression (Fig. 6D). Nevertheless, the downregulation of FOXM1 induced by inhibitors of AKT and ERK pathways was reversed in CKAP4-overexpression U87 and A172 cells (Fig. 6E). These data suggested CKAP4 positively regulates the expression of FOXM1 by activating the downstream AKT and ERK pathways.

Discussion

Specific normal, elevated, or mutational genes failed to be transcribed because of specific genetic factors, which might restrict research on genomics [36]. Numerous discrepancies between hub genes screened by RNA sequencing and proteomics provided information on protein expression research [37]. A view that proteins are the primary agents of biological processes provided insight into the molecular changes occurring in tumorigenesis or disease development. We aimed to explore the discrepant proteome profile of GBM and identify novel targets using high-throughput MS-based label-free quantitative proteomics. Based upon the bioinformatics approach, CKAP4 was identified as a key player in the malignant phenotype, and its role in positively regulating FOXM1 expression through activation of the AKT and ERK pathways was determined. Furthermore, using data from CGGA, a nomogram for prognosis in glioma patients based on CKAP4 expression and clinicopathologic features was constructed.

According to the proteomic analysis, the DEPs contain some of the major candidates previously identified to be involved in GBM development, such as overexpression of mitochondrial enzymes (Mn-superoxide dismutase, Mn-SOD) [38,39] and the cytoskeletal protein vimentin (VIM) [39,40]. Cytoskeletal proteins are among the most differentially expressed proteins in glioblastoma. A recent proteomic study found upregulated cytoskeletal expression (vimentin, α- and β-tubulin, β-actin and glial fibrillary acidic protein) in cells derived from GBM patients [38]. The migrative and invasive properties of GBM cells are associated with the shaping of the cytoskeleton. The capabilities of cancer cells to migrate and invade are promoted through the reorganization of

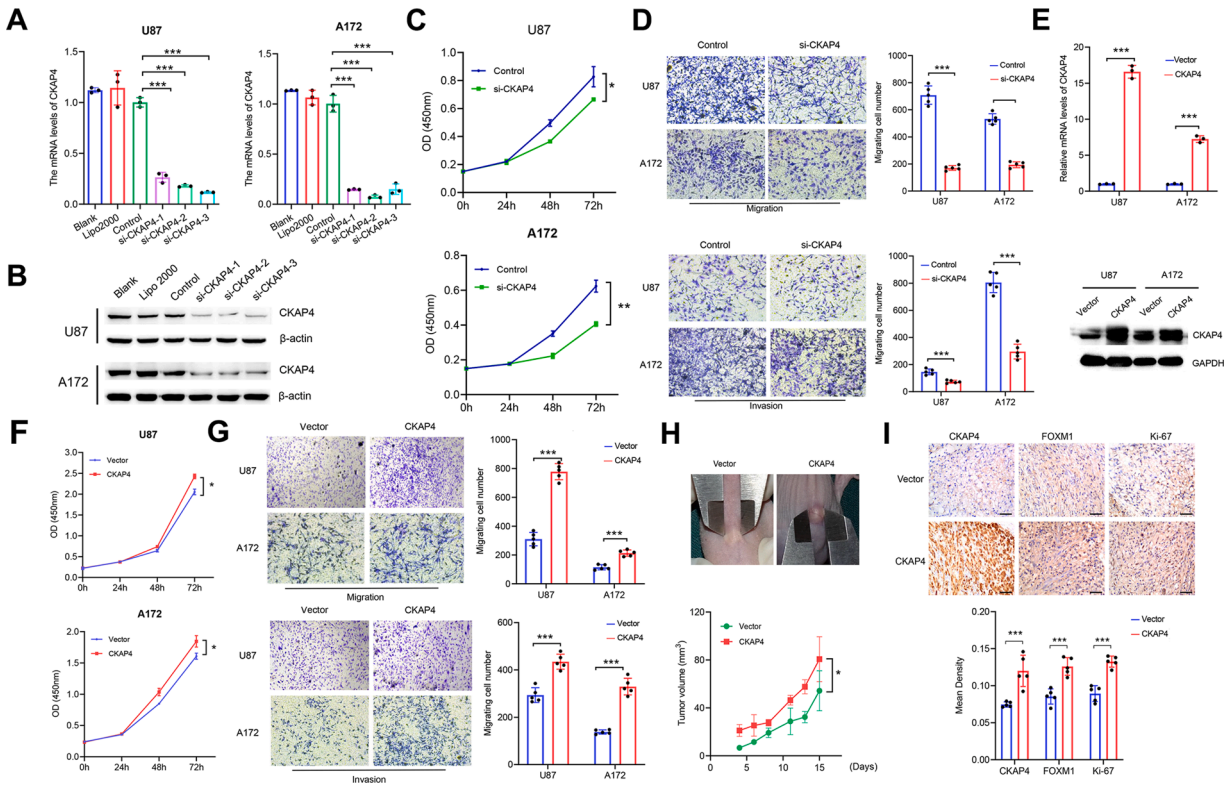

Fig. 4. Oncogenic capability of CKAP4 in GBM. (A) Effective elimination of CKAP4 mRNA and protein levels (B) in U87 and A172 cells determined by qPCR and western blot analysis, respectively. (C) The effect of CKAP4 knockdown on cell proliferation examined by the CCK8 assay. (D) Effects of CKAP4 knockdown on migration and invasion assessed by transwell assay. (Amplification: 40×). The representative pictures of migrated/invaded cells were shown in the up-panels, and statistical data of cell numbers were shown in the down-panels. The number of migrating cells that penetrated the transwell chamber is expressed as the mean number of cells from five random fields. Representative results from one experiment of three are shown. (E) Ectopic expression of CKAP4 in U87 and A172 cells determined by qPCR and western blot analysis. (F) Cell proliferation of CKAP4-overexpression and control cells. (G) Transwell assays were performed to evaluate migration or invasion capability in CKAP4-overexpression and control cells. (H) Representative pictures of xenograft tumors (left panel) and calculated results of tumor volumes in nude mice (right panel) from CKAP4-overexpression and control groups. (I) Ki-67 staining of xenograft tumors. The representative CKAP4, Ki-67 and FOXM1 staining were presented in U87 cell-derived xenograft tumors from CKAP4-overexpression and control mice (left panels). Histogram of the percentage of median density from five microscopic fields in each group (right panels). Data were shown as mean ± SD. Scale bar, 50 μm. *P < 0.05, **P < 0.01, ***P < 0.001.

cytoskeleton during the epithelial-mesenchymal transition [41]. Moreover, GBM also undergoes frequent biochemical alterations in the cytoskeletal regulatory network. It has been reported that BEX1 and BEX4 promoted the progression and radio-resistance of GBM cells through the formation of the filamentous cytoskeleton and subsequent activation of YAP (Yes-associated protein)/TAZ (transcriptional coactivator with PDZ-binding motif) signaling pathway [42]. Rhoj as a member of the Rho GTPase family interacts with moesin to promote proliferation and migration of GBM cells through activation of the Rac1/PAK pathway and actin remodeling [43]. A preliminary meta-analysis also showed that GBM was characterized by altered expression of cytoskeletal, with the cytoskeleton-associated protein 4 (CKAP4) screened as a potential key gene associated with GBM tumorigenesis included [44]. Docking studies further revealed that CKAP4 as a receptor binds to DKK1, further antagonizing Wnt signaling to disturb malignant behavior in tumorigenesis [45]. It was demonstrated that inhibiting Hippo signaling was one of the pathways by which CKPA4 was implicated in contributing to the malignant progression of gliomas [46]. Previous studies found that CKAP4 interacts with β1 integrin and regulates the recycling of α5β1 integrin independently of DKK1. The inhibition of CKAP4 on the recycling of α5β1 integrin further coordinates cell adhesion sites and migration [8]. A high level of expression of CKAP4 was also detected in our study of GBMs. Moreover, a large number of functional experiments also proved that CKAP4 facilitated tumorigenesis in GBM. Therefore, CKAP4 has the potential to be an effective biological target and its suppression might open an avenue of novel therapeutic strategy for GBM.

As a member of the FOX family, the essential proliferation-related transcription factor FOXM1 (Forkhead box protein M1) is spatiotemporally expressed in progenitor and regenerating tissues, tumor cells also included [47,48]. Considering that the decreased FOXM1 expression is rescued by the restoration of CKAP4 expression, we determined the regulatory effect of CKAP4 on FOXM1 expression [29], followed by illustrating its carcinogenesis in GBM. As was the case in previous studies [49–51], this study also detected an elevated expression of FOXM1 and CKAP4 in GBMs when compared to normal tissues. Our data displayed that CKAP4 activated FOXM1 expression at the post-transcriptional level. As supported, for patients with high levels of both CKAP4 and FOXM1, the survival probability was lower than that for those with either high or low expression of CKAP4 and FOXM1. Additionally, we discovered that CKAP4 promoted the malignant phenotype of GBM cells via FOXM1 activation.

As one of the crucial downstream target genes of Forkhead box O3 (FOXO3), FOXM1 expression and activation are negatively regulated directly at the transcriptional level [52]. Additionally, the AKT and ERK phosphorylation inhibits FOXO3 activity imposed by a prompt and sustained nuclear exclusion to the cytoplasm [53], which might further trigger the increased FOXM1 expression. We have demonstrated that the expression of FOXM1 was inhibited after U87 and A172 cells were treated with AKT inhibitor VIII or MEK inhibitor PD032590, and the effect of AKT inhibition and ERK inhibition on FOXM1 expression is synergistic. As uncovered by pathway enrichment analysis, CKAP4 is primarily involved in post-translational protein phosphorylation, and we indeed proved that overexpression of CKAP4 contributed to a high

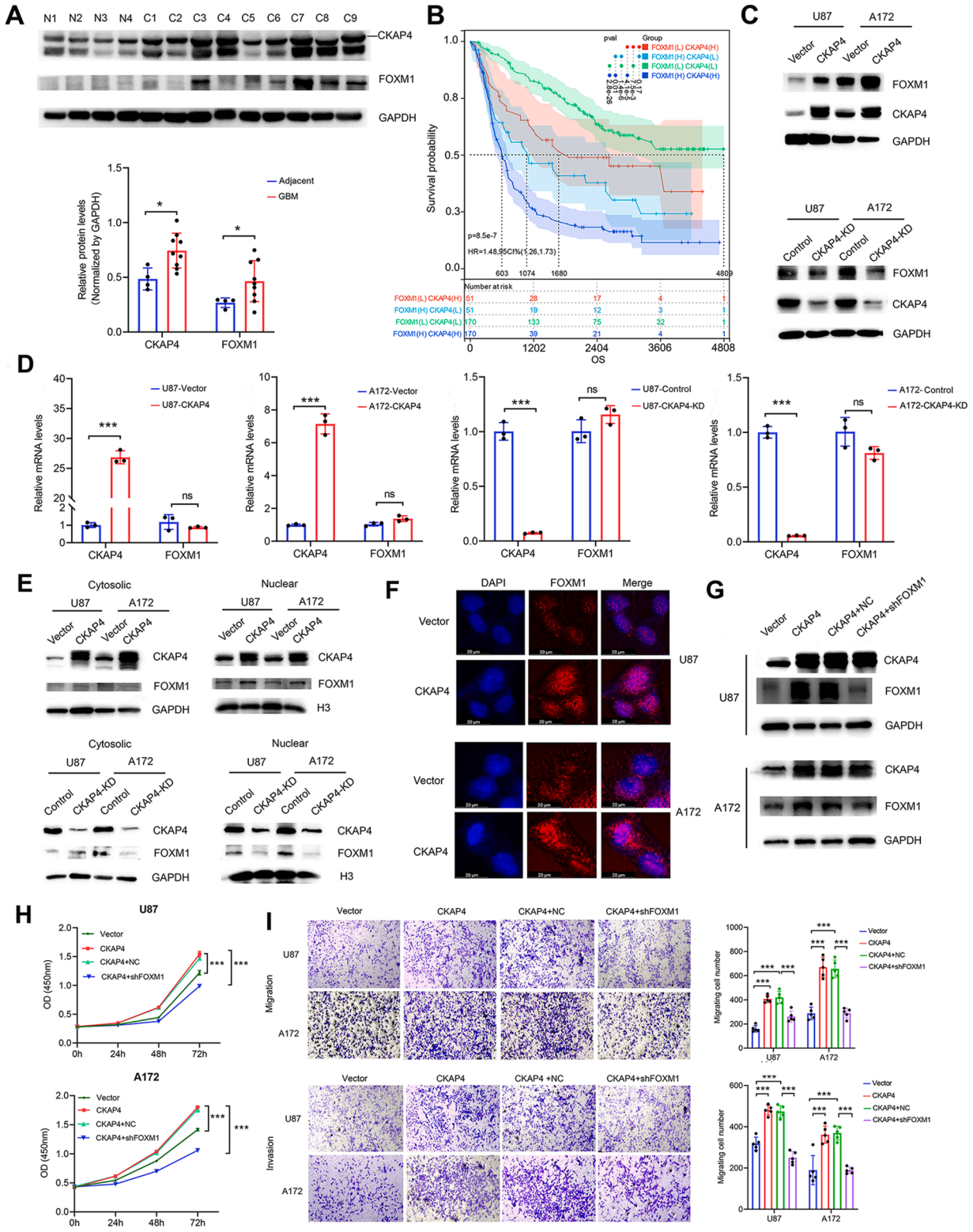

Fig. 5. CKAP4 regulates FOXM1 expression through post-transcriptional activation. (A) CKAP4 and FOXM1 expression were detected in GBM and adjacent tissue samples (up-panels). Statistical data were shown in the down-panels. (B) The correlation between CKAP4 and FOXM1 expression and overall survival (OS) in patients with gliomas (data integrated from CGGA datasets). (C) FOXM1 expression was evaluated in CKAP4 overexpression-U87 and A172 cells by western blot and qPCR (D). GAPDH was used as the normalized controls. (E) FOXM1 expression in the cytosolic and nuclear fractions was detected. GAPDH and Histone H3 were used for loading controls, respectively. (F) The effect of CKAP4 overexpression on FOXM1 localization was determined by immunofluorescence in CKAP4 overexpression-U87 (up) and A172 cells (Down). (G) The efficient removal of FOXM1 protein levels in U87 and A172 cells overexpressing CKAP4 was measured by western blot. (H) CCK8 assay was utilized to assess the ability to proliferate, and transwell assay (I) was used to assess the capacity to migrate and invade in U87 and A172 cells that were stably expressing CKAP4. All data were shown as mean ± SD. *P < 0.05, **P < 0.01, ***P < 0.001.

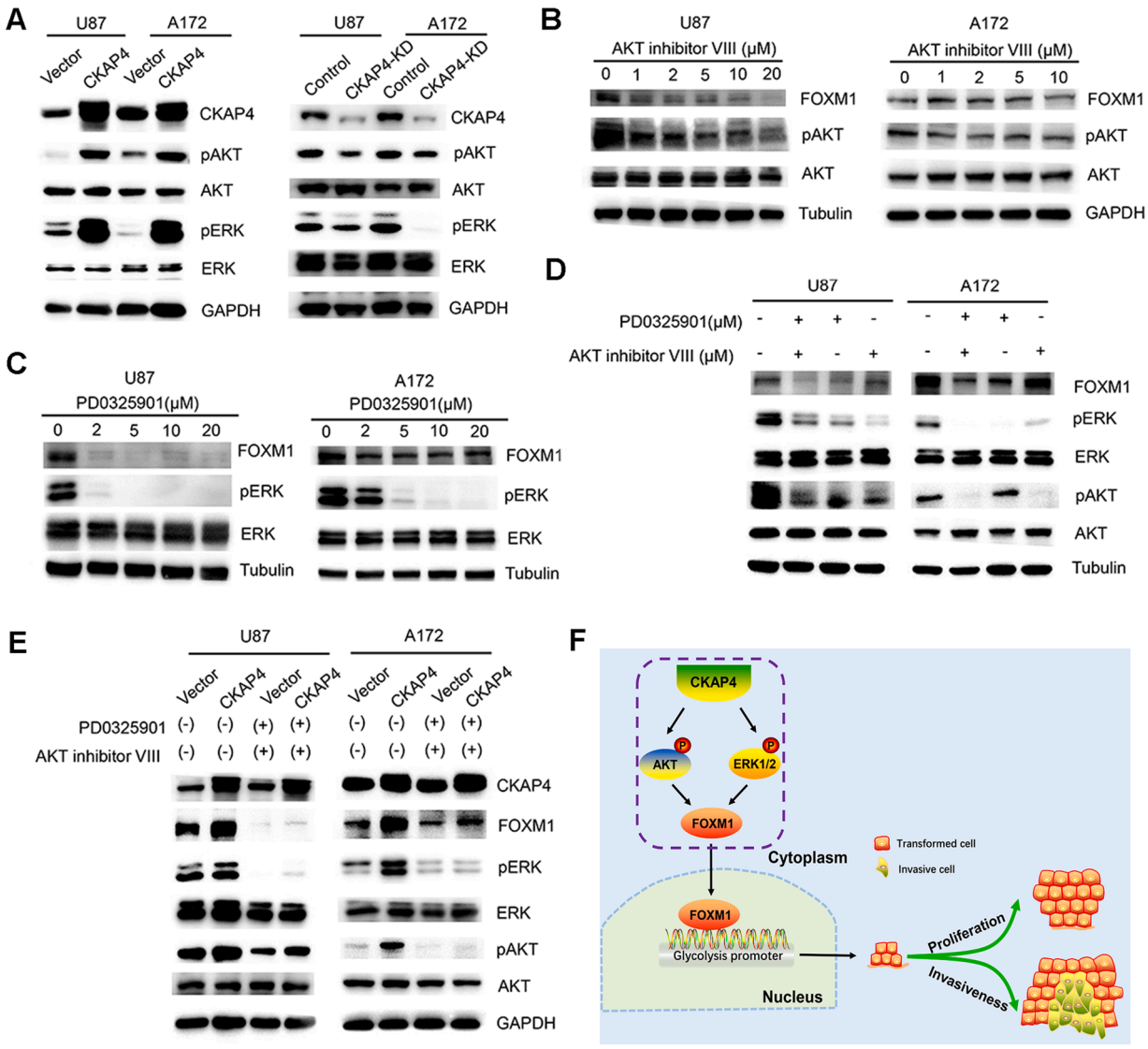

Fig. 6. CKAP4 modulates FOXM1 expression through the AKT/ERK signaling pathway. (A) Lysates of control and stably CKAP4-overexpressed or CKAP4-knocldown U87 and A172 cells were probed with the indicated antibodies. KD: Knockdown. (B) U87 and A172 cells were treated with different concentration of AKT inhibitor VIII and PD0325901 for 48 h, and the lysates were then probed with the appropriate antibodies. (C) U87 and A172 cells were simultaneously treated with AKT inhibitor VIII (20 μM and 10 μM, respectively) and PD0325901 (2 μM) for 48 h, and the lysates were then probed with the indicated antibodies. (D) U87 and A172 cells stably expressing CKAP4 were treated with both inhibitor VIII and PD0325901 for 48 h. Lysates were incubated with indicated antibodies, followed by detection. (E) A schematic diagram for CKAP4 promoting malignant phenotypes in GBM. In glioblastoma cells, CKAP4-mediated FOXM1 activation via phosphorylation pathways regulates malignant behavior of glioblastoma cells.

level of phosphorylated AKT and ERK. Based on the above results, we hypothesized that CKAP4 might modulate FOXM1 expression through the activation of AKT and ERK. As supported, our data showed CKAP4 reversed the downregulation of FOXM1 caused by AKT and ERK inhibitors. Although the AKT and MEK inhibitors had no significant influence on CKAP4 expression, the inhibition effects on FOXM1 might antagonize the oncogenic phenotype caused by CKAP4 overexpression. At present, the kinase pathways have been identified as prospective therapeutic targets. A novel AKT inhibitor SC66 exerts prominently antitumor efficiency in vivo and in vitro, contributing to its potential applications for the valid treatment of GBM [54]. Inhibitors with improved pharmacokinetics have been considered for the design and development of anticancer agents to improve the prognosis of GBM.

Furthermore, a nomogram for predicting the survival probability among glioma patients integrated more parameters including CKAP4 expression, exhibiting an excellent discriminative ability and universal clinical applicability. Based on CKAP4 expression analysis and other parameters, the nomogram was applied to calculate a total score that can predict prognosis. To some extent, integrating the quantified and visual predictive scoring system can provide some guidance or reference for clinicians to make more objective treatment options. For patients with high scores meant adverse outcomes and therapeutic regimes including drugs or inhibitors that block CKAP4-involved pathways would be adopted. Considering the inhibition effect of AKT and EKR inhibitors on CKAP4 over-expressed GBM cells, preclinical studies on the efficacy of kinase inhibitors or combined with anti-CKAP4 drugs in GBM deserve attention and further studying.

Conclusion

A brief overview of our findings is that we used proteomics profiling to identify CKAP4 as an oncogene in GBM, and that we demonstrated for the first time that CKAP4 modulated malignant behaviors through activation of FOXM1 via downstream signaling mechanisms, such as

AKT and ERK. In addition, we developed a nomogram for predicting the risk and likelihood of survival of patients diagnosed with gliomas. We anticipate that the present study will provide considerable insight into complex biochemical processes and GBM biology, as well as provide more accurate risk predictions for gliomas.

Author contribution

KX performed data processing and manuscript drafting. **CC, HW and LW** contributed to the study design and revision of the manuscript. **KZ, JM, QY and GY** contributed to the data collection and processing. **TZ, GW and BY** provided the administrative, technical, and material support. **JS** conducted the bioinformatics analysis. All authors made substantial intellectual contributions to this study and reviewed and approved the final version of the manuscript.

Funding

This work was supported by the Basic Research Program of Natural Sciences of Shaanxi Province (2023-JC-YB-712) and Xi'an Talent Program (XAYC210032).

Declaration of Competing Interests

The authors declare that they have no known competing financial interests or personal relationships that could have appeared to influence the work reported in this paper.

References

[1] DN Louis, H Ohgaki, OD Wiestler, et al., The 2007 WHO classification of tumours of the central nervous system, Acta Neuropathol. 114 (2) (2007) 97–109.
[2] R Stupp, S Taillibert, A Kanner, et al., Effect of tumor-treating fields plus maintenance temozolomide vs maintenance temozolomide alone on survival in patients with glioblastoma: A randomized clinical trial, JAMA 318 (23) (2017) 2306–2316.
[3] CC Poon, S Sarkar, VW Yong, et al., Glioblastoma-associated microglia and macrophages: targets for therapies to improve prognosis, Brain 140 (6) (2017) 1548–1560.
[4] ME Hegi, A-C Diserens, T Gorlia, et al., MGMT gene silencing and benefit from temozolomide in glioblastoma, N. Engl. J. Med. 352 (10) (2005) 997–1003.
[5] RJ Komotar, ML Otten, G Moise, et al., Radiotherapy plus concomitant and adjuvant temozolomide for glioblastoma-a critical review, Clin. Med. Oncol. 2 (2008) 421–422.
[6] R Stupp, ME Hegi, WP Mason, et al., Effects of radiotherapy with concomitant and adjuvant temozolomide versus radiotherapy alone on survival in glioblastoma in a randomised phase III study: 5-year analysis of the EORTC-NCIC trial, Lancet Oncol. 10 (5) (2009) 459–466.
[7] A Schweizer, M Ericsson, T Bächi, et al., Characterization of a novel 63 kDa membrane protein. Implications for the organization of the ER-to-Golgi pathway, J. Cell Sci. 104 (Pt 3) (1993) 671–683.
[8] Y Osugi, K Fumoto, A Kikuchi, CKAP4 regulates cell migration via the interaction with and recycling of integrin, Mol. Cell. Biol. 39 (16) (2019) e00073-00019.
[9] N Gupta, Y Manevich, AS Kazi, et al., Identification and characterization of p63 (CKAP4/ERGIC-63/CLIMP-63), a surfactant protein A binding protein, on type II pneumocytes. American journal of physiology, Am. J. Physiol. Lung Cell. Mol. Physiol. 291 (3) (2006) L436–L446.
[10] L Gao, Q Wang, W Ren, et al., The RBP1-CKAP4 axis activates oncogenic autophagy and promotes cancer progression in oral squamous cell carcinoma, Cell Death. Dis. 11 (6) (2020) 488.
[11] N Shinno, H Kimura, R Sada, et al., Activation of the Dickkopf1-CKAP4 pathway is associated with poor prognosis of esophageal cancer and anti-CKAP4 antibody may be a new therapeutic drug, Oncogene 37 (26) (2018) 3471–3484.
[12] GF Lu, CY You, YS Chen, et al., MicroRNA-671-3p promotes proliferation and migration of glioma cells via targeting CKAP4, Onco. Targets Ther. 11 (2018) 6217–6226.
[13] CM Sun, J Geng, Y Yan, et al., Overexpression of CKAP4 is associated with poor prognosis in clear cell renal cell carcinoma and functions via cyclin B signaling, J. Cancer 8 (19) (2017) 4018–4026.
[14] H Kimura, K Fumoto, K Shojima, et al., CKAP4 is a Dickkopf1 receptor and is involved in tumor progression, J. Clin. Invest. 126 (7) (2016) 2689–2705.
[15] C Kajiwara, K Fumoto, H Kimura, et al., p63-dependent Dickkopf3 expression promotes esophageal cancer cell proliferation via CKAP4, Cancer Res. 78 (21) (2018) 6107–6120.
[16] A Kikuchi, K Fumoto, H Kimura, The Dickkopf1-cytoskeleton-associated protein 4 axis creates a novel signaling pathway and may represent a molecular target for cancer therapy, Br. J. Pharmacol. 174 (24) (2017) 4651–4665.
[17] H Kimura, H Yamamoto, T Harada, et al., CKAP4, a DKK1 receptor, is a biomarker in exosomes derived from pancreatic cancer and a molecular target for therapy, Clin. Cancer Res. 25 (6) (2019) 1936–1947.
[18] Y-B Pan, S Wang, B Yang, et al., Transcriptome analyses reveal molecular mechanisms underlying phenotypic differences among transcriptional subtypes of glioblastoma, J. Cell. Mol. Med. 24 (7) (2020) 3901–3916.
[19] HJ Park, G Gusarova, Z Wang, et al., Deregulation of FoxM1b leads to tumour metastasis, EMBO Mol. Med. 3 (1) (2011) 21–34.
[20] Y Wang, B Yao, Y Wang, et al., Increased FoxM1 expression is a target for metformin in the suppression of EMT in prostate cancer, Int. J. Mol. Med. 33 (6) (2014) 1514–1522.
[21] S Yao, LY Fan, EW Lam, The FOXO3-FOXM1 axis: A key cancer drug target and a modulator of cancer drug resistance, Semin. Cancer Biol. 50 (2018) 77–89.
[22] S Zona, L Bella, MJ Burton, et al., FOXM1: an emerging master regulator of DNA damage response and genotoxic agent resistance, Biochim. Biophys. Acta 1839 (11) (2014) 1316–1322.
[23] I Wierstra, FOXM1 (Forkhead box M1) in tumorigenesis: overexpression in human cancer, implication in tumorigenesis, oncogenic functions, tumor-suppressive properties, and target of anticancer therapy, Adv. Cancer. Res. 119 (2013) 191–419.
[24] R Shang, M Wang, B Dai, et al., Long noncoding RNA SLC2A1-AS1 regulates aerobic glycolysis and progression in hepatocellular carcinoma via inhibiting the STAT3/FOXM1/GLUT1 pathway, Mol. Oncol. 14 (6) (2020) 1381–1396.
[25] Y Wang, Y Yun, B Wu, et al., FOXM1 promotes reprogramming of glucose metabolism in epithelial ovarian cancer cells via activation of GLUT1 and HK2 transcription, Oncotarget 7 (30) (2016) 47985–47997.
[26] J Cui, M Shi, D Xie, et al., FOXM1 promotes the warburg effect and pancreatic cancer progression via transactivation of LDHA expression, Clin. Cancer Res. 20 (10) (2014) 2595–2606.
[27] TW Kim, HH Ryu, SY Li, et al., PDIA6 regulation of ADAM17 shedding activity and EGFR-mediated migration and invasion of glioblastoma cells, J. Neurosurg. 126 (6) (2017) 1829–1838.
[28] Q Chen, B Han, X Meng, et al., Immunogenomic analysis reveals LGALS1 contributes to the immune heterogeneity and immunosuppression in glioma, Int. J. Cancer 145 (2) (2019) 517–530.
[29] H Kimura, R Sada, N Takada, et al., The Dickkopf1 and FOXM1 positive feedback loop promotes tumor growth in pancreatic and esophageal cancers, Oncogene 40 (26) (2021) 4486–4502.
[30] X Su, Y Yang, Q Yang, et al., NOX4-derived ROS-induced overexpression of FOXM1 regulates aerobic glycolysis in glioblastoma, BMC Cancer 21 (1) (2021) 1181.
[31] EA Partridge, C Le Roy, GM Di Guglielmo, et al., Regulation of cytokine receptors by Golgi N-glycan processing and endocytosis, Science 306 (5693) (2004) 120–124.
[32] OM Ijomone, JD Iroegbu, M Aschner, et al., Impact of environmental toxicants on p38- and ERK-MAPK signaling pathways in the central nervous system, Neurotoxicology 86 (2021) 166–171.
[33] HJ Park, JR Carr, Z Wang, et al., FoxM1, a critical regulator of oxidative stress during oncogenesis, EMBO J. 28 (19) (2009) 2908–2918.
[34] L Yang, S Xie, MS Jamaluddin, et al., Induction of androgen receptor expression by phosphatidylinositol 3-kinase/Akt downstream substrate, FOXO3a, and their roles in apoptosis of LNCaP prostate cancer cells, J. Biol. Chem. 280 (39) (2005) 33558–33565.
[35] RY Ma, TH Tong, AM Cheung, et al., Raf/MEK/MAPK signaling stimulates the nuclear translocation and transactivating activity of FOXM1c, J. Cell Sci. 118 (Pt 4) (2005) 795–806.
[36] G Lubec, K Krapfenbauer, M Fountoulakis, Proteomics in brain research: potentials and limitations, Prog. Neurobiol. 69 (3) (2003) 193–211.
[37] TC Network. Corrigendum, Comprehensive genomic characterization defines human glioblastoma genes and core pathways, Nature 494 (7438) (2013) 506.
[38] B Collet, N Guitton, S Saïkali, et al., Differential analysis of glioblastoma multiforme proteome by a 2D-DIGE approach, Proteome Sci. 9 (1) (2011) 16.
[39] RF Deighton, T Le Bihan, SF Martin, et al., Interactions among mitochondrial proteins altered in glioblastoma, J. Neurooncol. 118 (2) (2014) 247–256.
[40] RV Polisetty, P Gautam, R Sharma, et al., LC-MS/MS analysis of differentially expressed glioblastoma membrane proteome reveals altered calcium signaling and other protein groups of regulatory functions, Mol. Cell. Proteomics 11 (6) (2012), M111.013565.
[41] M Yilmaz, G Christofori, EMT, the cytoskeleton, and cancer cell invasion, Cancer Metastasis Rev. 28 (1-2) (2009) 15–33.
[42] S Lee, H Kang, E Shin, et al., BEX1 and BEX4 induce GBM progression through regulation of actin polymerization and activation of YAP/TAZ signaling, Int. J. Mol. Sci. 22 (18) (2021) 9845.
[43] M Wang, X Jiang, Y Yang, et al., Rhoj is a novel target for progression and invasion of glioblastoma by impairing cytoskeleton dynamics, Neurotherapeutic 17 (4) (2020) 2028–2040.
[44] F Grespi, C Vianello, S Cagnin, et al., The interplay of microtubules with mitochondria-ER contact sites (MERCs) in glioblastoma, Biomolecules 12 (4) (2022) 567.
[45] C Niehrs, Function and biological roles of the Dickkopf family of Wnt modulators, Oncogene 25 (57) (2006) 7469–7481.
[46] T Luo, K Ding, J Ji, et al., Cytoskeleton-associated protein 4 (CKAP4) promotes malignant progression of human gliomas through inhibition of the Hippo signaling pathway, J. Neuroncol. 154 (3) (2021) 275–283.
[47] GB Liao, XZ Li, S Zeng, et al., Regulation of the master regulator FOXM1 in cancer, Cell Commun. Signal: CCS 16 (1) (2018) 57.

[48] D Nandi, PS Cheema, N Jaiswal, et al., FoxM1: Repurposing an oncogene as a biomarker, Semin. Cancer Biol. 52 (Pt 1) (2018) 74–84.
[49] M Liu, B Dai, SH Kang, et al., FoxM1B is overexpressed in human glioblastomas and critically regulates the tumorigenicity of glioma cells, Cancer Res. 66 (7) (2006) 3593–3602.
[50] Y Lee, KH Kim, DG Kim, et al., FoxM1 promotes stemness and radio-resistance of glioblastoma by regulating the master stem cell regulator Sox2, PLoS One 10 (10) (2015), e0137703.
[51] H Wu, M Wei, Y Li, et al., Research progress on the regulation mechanism of key signal pathways affecting the prognosis of glioma, Front. Mol. Neurosci. 15 (2022), 910543.
[52] CT Karadedou, AR Gomes, J Chen, et al., Correction: FOXO3a represses VEGF expression through FOXM1-dependent and -independent mechanisms in breast cancer, Oncogene 38 (25) (2019) 5111–5112.
[53] J Nakae, T Kitamura, Y Kitamura, et al., The forkhead transcription factor Foxo1 regulates adipocyte differentiation, Dev. Cell 4 (1) (2003) 119–129.
[54] L Gao, J Liu, P Xu, et al., AKT inhibitor SC66 inhibits proliferation and induces apoptosis in human glioblastoma through down-regulating AKT/β-Catenin pathway, Front. Pharmacol. 11 (2020) 1102.